Magnetic structure of $CeRhIn_5$ under magnetic field

2007 J. Phys.: Condens. Matter 19 242204

(http://iopscience.iop.org/0953-8984/19/24/242204)

IOP FTC

IOP PUBLISHING JOURNAL OF PHYSICS: CONDENSED MATTER

J. Phys.: Condens. Matter **19** (2007) 242204 (8pp) doi:10.1088/0953-8984/19/24/242204

FAST TRACK COMMUNICATION

Magnetic structure of $CeRhIn_5$ under magnetic field

S Raymond, E Ressouche, G Knebel, D Aoki and J Flouquet

CEA-Grenoble, DRFMC, SPSMS, 38054 Grenoble Cedex 9, France

Received 10 April 2007, in final form 10 May 2007
Published 24 May 2007
Online at stacks.iop.org/JPhysCM/19/242204

Abstract

The magnetically ordered ground state of $CeRhIn_5$ at ambient pressure and zero magnetic field is an incommensurate helicoidal phase with the propagation vector $\mathbf{k} = (1/2, 1/2, 0.298)$ and the magnetic moment in the basal plane of the tetragonal structure. We determined by neutron diffraction the two different magnetically ordered phases of $CeRhIn_5$ evidenced by bulk measurements under applied magnetic field in the basal plane. The low temperature high magnetic phase corresponds to a commensurate sine-wave structure of the magnetization with $\mathbf{k} = (1/2, 1/2, 1/4)$. At high temperature, the phase is incommensurate with $\mathbf{k} = (1/2, 1/2, 0.298)$ and a possible small ellipticity. The propagation vector of this phase is the same as that of the zero-field structure.

The interplay between magnetism and superconductivity is one of the most important points of interest in the study of heavy fermion systems [1]. A widely open question concerns the cooperative versus antagonist nature of the two ground states. The generic phase diagram obtained in heavy fermion systems, high-T_c superconductors and organics is composed of a superconducting region appearing in the vicinity of a vanishing magnetic phase. Because magnetic fluctuations are expected to be strong in this region of the phase diagram, they are invoked as responsible for the Cooper pair formation [2]. However, no definitive agreement between experiment and theory firmly establishes this point in the same manner that the classical scenario of phonon mediated pairing does for conventional superconductivity. In contrast, the SO(5) theory describes the two phenomena, magnetism and superconductivity, in a unified picture via a superspin order parameter that encompasses both states [3]. This leads to a rich variety of possible phase diagrams with so far limited examples to test experimentally this theory in detail [4]. In this respect, $CeRhIn_5$ (and the related $CeTIn_5$ compounds with T = Ir and Co [5]) provides a unique experimental case, where the Néel temperature (T_N) and the superconducting transition temperature (T_c) are of the same order (of about 1 K) and can be tuned by pressure (p) or magnetic field (H). The resulting intricate magnetic and superconducting (p, T, H) phase diagram of $CeRhIn_5$ points towards competition between antiferromagnetism and superconductivity [6–8]: at zero magnetic field, there is a pressure range (1.6–1.9 GPa) where magnetism and superconductivity coexist with $T_N > T_c$. Above

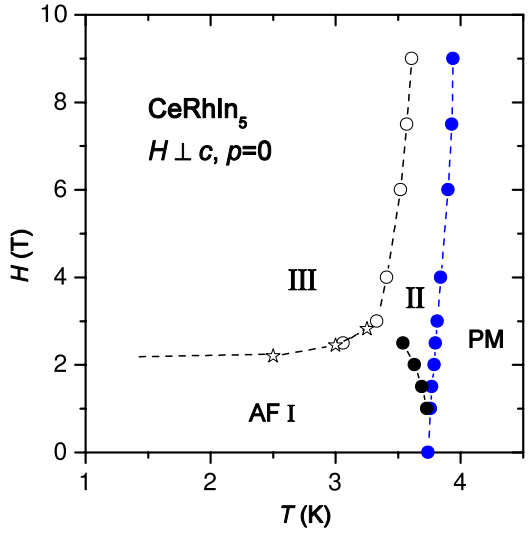

Figure 1. (T, H) phase diagram of $CeRhIn_5$ determined by specific heat for field applied in the basal plane at ambient pressure. It shows three different ordered phases. Open (full) symbols correspond to first (second) order transition.

(This figure is in colour only in the electronic version)

2 GPa, where $T_N \approx T_c$, a pure superconducting phase emerges and antiferromagnetism is suppressed. The application of a magnetic field in this phase induces a spectacular re-entrance of the long range magnetic order. Apart from NMR experiments [9], microscopic probes are lacking to address the nature of the magnetically ordered phases in the (p, T, H) phase diagram. To this end, and as a starting point for further investigations to be performed under pressure, we have investigated the magnetically ordered phases of $CeRhIn_5$ under magnetic field applied in the basal plane at zero pressure.

$CeRhIn_5$ crystallizes in the tetragonal space group $P4/mmm$ [10]. The sample was obtained by the In self-flux method. A rectangular-shaped platelet of width 1 mm normal to the c-axis was cut from this batch, the other dimensions being 4.3 mm along [1, $\overline{1}$, 0] and 2.7 mm along [1, 1, 0]. This geometry is chosen to minimize the strong absorption cross section from In and Rh for the study of the ([1, 1, 0], [0, 0, 1]) scattering plane. The measurements were performed on the two-axis D23-CEA-CRG (Collaborating Research Group) thermal-neutron diffractometer equipped with a lifting detector at the Institut Laue Langevin (ILL), Grenoble. A copper monochromator provides an unpolarized beam with a wavelength of $\lambda = 1.276$ Å. The sample was mounted in a vertical field ^{4}He flow cryomagnet with the [1, $\overline{1}$, 0] axis along the magnetic field.

The (T, H) phase diagram obtained by calorimetry measurements for the field applied perpendicular to the tetragonal axis is shown in figure 1. It is composed of three magnetically ordered phases (two being induced by the magnetic field) consistently with the data obtained by other groups using calorimetry [11], thermal expansion and magnetostriction [12]. In the diffraction experiment, we apply the field along [1, $\overline{1}$, 0] and refer to this phase diagram by neglecting the in-plane anisotropy. The magnetic structure at zero field is known to be incommensurate with slightly different propagation vectors reported in the literature, $\mathbf{k} = (1/2, 1/2, 0.297)$ [13] or $\mathbf{k} = (1/2, 1/2, 0.298)$ [14]. The helicoidal nature of the order, as opposed to a sine-wave modulated structure, is known from the distribution of the hyperfine field observed in NQR measurements [15].

Table 1. Structural parameters at $T = 1.9$ K. (Note: $R = 0.0532$.)

$a = 4.638$ Å $c = 7.521$ Å	
z	0.305 26 (14)
u_{Ce}	0.0014 (5) Å^2
u_{Rh}	0.0006 (4) Å^2
u_{In1}	0.0018 (5) Å^2
u_{In2}	0.0015 (4) Å^2

In this paper, all refinements of the crystal and magnetic structures were performed using the software MXD [16]. The extinction correction was made using the Becker Coppens method [17] and absorption correction was taken into account with the linear absorption coefficient $\mu = 0.49$ mm^{-1}. For each refinement, the weighted least square factor R is given. Its expression is $R = \sqrt{\sum[(I_{\mathrm{obs}} - I_{\mathrm{calc}})/\sigma_{I_{\mathrm{obs}}}]^2 / \sum[I_{\mathrm{obs}}/\sigma_{I_{\mathrm{obs}}}]^2}$, where I_{obs} and I_{calc} are the observed and calculated (nuclear or magnetic) intensities and $\sigma_{I_{\mathrm{obs}}}$ is the standard deviation. In the present experiment, the lattice parameters were obtained from the centring of 18 independent reflections of the crystal and a refinement of the nuclear structure was performed at 1.9 K with 181 Bragg peaks yielding the structural parameters shown in table 1 and the scale factor for the magnetic structure calculation. These parameters are consistent with those of the literature concerning the lattice parameters and the fractional coordinate z [10]. The principal mean square atomic displacements u have typical values for such intermetallic compounds. As far as magnetic scattering is concerned, the measured neutron Bragg intensity after correction for scale factor, extinction, absorption and Lorentz factor is the square of the component of the magnetic structure factor perpendicular to $\mathbf{Q}$:$|\mathbf{F}_{\mathrm{M}\perp}(\mathbf{Q})|^2$. In the present case with only one magnetic Ce atom/unit cell at the origin, the magnetic structure factor is

$$\mathbf{F}_{\mathrm{M}}(\mathbf{Q}) = pf(\mathbf{Q})\mathbf{m}_{\mathbf{k}}\mathrm{e}^{-W_{\mathrm{Ce}}} \tag{1}$$

where $p \approx 0.27 \times 10^{-12}$ cm is the scattering amplitude at $Q = 0$ for a single magnetic moment of 1 μ_{B}, $f(\mathbf{Q})$ is the Ce magnetic form factor and W_{Ce} is the Debye–Waller factor of Ce. $\mathbf{m}_{\mathbf{k}}$ is the Fourier component of the magnetic moment distribution. The magnetic structures of interest for the present paper are (i) the collinear sine-wave structure, for which

$$\mathbf{m}_{\mathbf{k}} = \frac{A_k}{2}\mathbf{u}_{\mathbf{k}}\mathrm{e}^{\mathrm{i}\Phi_k} \tag{2}$$

and (ii) the non-collinear elliptical structure:

$$\mathbf{m}_{\mathbf{k}} = \tfrac{1}{2}(m^u\mathbf{u}_{\mathbf{k}} + \mathrm{i}m^v\mathbf{v}_{\mathbf{k}})\mathrm{e}^{\mathrm{i}\Phi_k} \tag{3}$$

where A_k is the amplitude of the sine wave, $\mathbf{u}_{\mathbf{k}}$ and $\mathbf{v}_{\mathbf{k}}$ are unit vectors, Φ_k is a phase factor and m^u, m^v are the components of the magnetic moment along the unit vectors $\mathbf{u}_{\mathbf{k}}$ and $\mathbf{v}_{\mathbf{k}}$. The helicoidal order corresponds to the particular case $m^u = m^v$.

The obtained propagation vector for the zero-field magnetic structure is found to be $\mathbf{k} = (1/2, 1/2, 0.298)$, in agreement with the literature. The structure was determined by measuring 16 magnetic peaks and by performing a least square fitting of the helicoidal model. The comparison between the observed intensities and the calculated ones is shown in table 2. A magnetic moment $m_{\mathrm{I}} = 0.59(1)$ μ_{B} is found at 1.9 K, a value a little lower than the one found in the literature, 0.75(2) μ_{B} at 1.4 K [13]. Given the rather flat temperature evolution of the order parameter between 1.4 and 1.9 K [13], the difference in the magnetic moment determination is not due to the difference in the measurement temperature. We believe that this

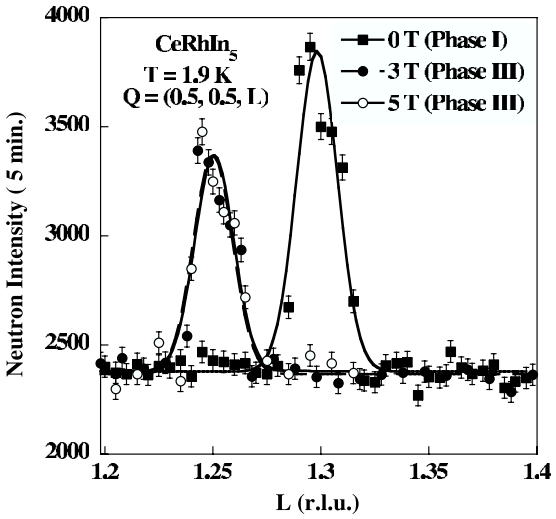

Figure 2. **Q**-scans performed along the c-axis for $H = 0$, 3 and 5 T at 1.9 K.

Table 2. Magnetic refinement with a helicoidal structure at zero field in phase I at $T = 1.9$ K. The **Q** vector is the Brillouin zone centre +/− the propagation vector $\mathbf{k} = (1/2, 1/2, 0.298)$. (Note: $R = 0.0696$.)

Q	$\lvert\mathbf{F}_{M\perp}(\mathbf{Q})\rvert^2_{calc}$	$\lvert\mathbf{F}_{M\perp}(\mathbf{Q})\rvert^2_{obs}$
(1, 1, 0)−	1.10	1.17 (0.03)
(0, 0, 0)+	1.10	1.03 (0.05)
(0, 0, 1)+	1.52	1.50 (0.06)
(−1, −1, 1)+	1.52	1.39 (0.06)
(0, −1, 1)+	1.52	1.43 (0.09)
(1, 1, 1)−	1.30	1.36 (0.05)
(1, 1, 1)+	0.76	0.46 (0.12)
(0, 0, 2)+	1.54	1.50 (0.07)
(1, 1, 2)−	1.57	1.63 (0.06)
(0, 0, 2)−	1.57	1.53 (0.06)
(1, 0, 2)−	1.57	1.47 (0.09)
(2, 2, 2)−	0.78	0.57 (0.22)
(1, 1, 3)−	1.47	1.62 (0.09)
(0, 0, 4)+	1.08	1.34 (0.12)
(1, 1, 4)−	1.24	1.14 (0.20)
(1, 1, 5)−	0.97	0.94 (0.11)

difference is related to the data treatment, the present work including absorption and extinction corrections.

Figure 2 show **Q**-scans performed along the c-axis for $H = 3$ and 5 T (phase III) with the same scan performed at $H = 0$ T as a reference (phase I). The propagation vector is now commensurate being $(1/2, 1/2, 1/4)$. For this phase, seven magnetic reflections were collected at $H = 3$ T and $T = 1.9$ K. The best refinement is obtained for a collinear sine-wave structure (see table 3) with the moment perpendicular to the field, i.e. along [1, 1, 0]. Refinement with a helical structure does not work. For completeness, an elliptic structure was refined and yields, within the error bars, zero component of the magnetic moment along the

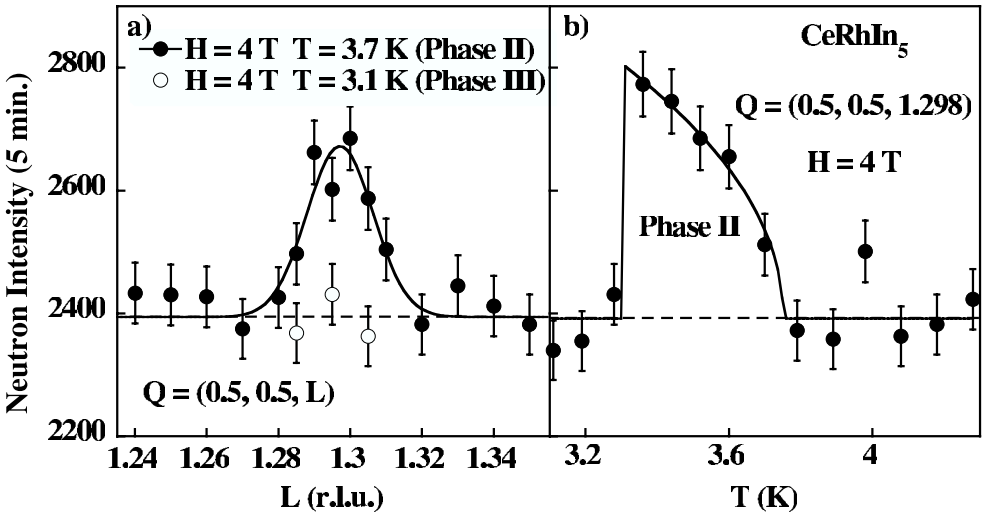

Figure 3. (a) **Q**-scans performed along the c-axis for $H = 4$ T at 3.1 and 3.7 K. (b) Temperature dependence of the Bragg peak intensity at $\mathbf{Q} = (0.5, 0.5, 1.295)$ for $H = 4$ T. Solid lines are guides for the eyes. The dashed line represents the background.

Table 3. Magnetic refinement with a sine-wave structure in phase III for $H = 3$ T and $T = 1.9$ K. (Note: $R = 0.0934$.)

Q	$\lvert\mathbf{F}_{M\perp}(\mathbf{Q})\rvert^2_{calc}$	$\lvert\mathbf{F}_{M\perp}(\mathbf{Q})\rvert^2_{obs}$
(0, 0, 1)+	1.08	1.02 (0.07)
(1, 1, 1)−	0.62	0.65 (0.05)
(0, 0, 2)+	1.40	1.42 (0.09)
(1, 1, 2)−	1.32	1.31 (0.06)
(1, 1, 3)−	1.38	1.30 (0.14)
(0, 0, 4)+	1.08	1.00 (0.12)
(1, 1, 4)−	1.19	1.82 (0.20)

field and thus confirms the sine-wave refinement. The propagation vector $\mathbf{k} = (1/2, 1/2, 1/4)$ corresponds to a particular case of the sine wave. For a phase $\Phi_k = -\pi/4$ in equation (2), all the magnetic moments have the same length and the magnetic structure corresponds to the so-called $++--$ structure consisting of an up, up, down, down sequence of magnetic moment when moving along the c-axis. This structure is favoured at low temperature because it reduces the magnetic entropy. The obtained magnetic amplitude of the sine wave at 1.9 K is $A_{III} = 0.84(2)\ \mu_B$. For the peculiar $++--$ structure, the magnetic moment m_{III} is related to the sine-wave amplitude by $m_{III} = A_{III}/\sqrt{2}$. We thus obtain $m_{III} = 0.59\ \mu_B$, the same value as m_I. Note that the maximum in plane magnetic moment expected on the doublet ground state is 0.92 μ_B as deduced from crystal field spectroscopy [18]. The difference between the paramagnetic moment of the doublet ground state and the saturated ordered moment is often ascribed to the Kondo effect in cerium compounds.

Phase II was investigated by performing **Q**-scans at 3.7 K and 4 T. An example of such a scan along the c-axis is shown in figure 3(a) for $\mathbf{Q} = (0.5, 0.5, L)$, with the same scan performed at 3.1 K in phase III as a reference. The propagation vector is found to be the same as for the helicoidal phase, i.e. $\mathbf{k} = (1/2, 1/2, 0.298)$. Figure 3(b) shows the temperature variation of the magnetic Bragg peak $\mathbf{Q} = (0.5, 0.5, 1.298)$ at 4 T. The difficulty of studying

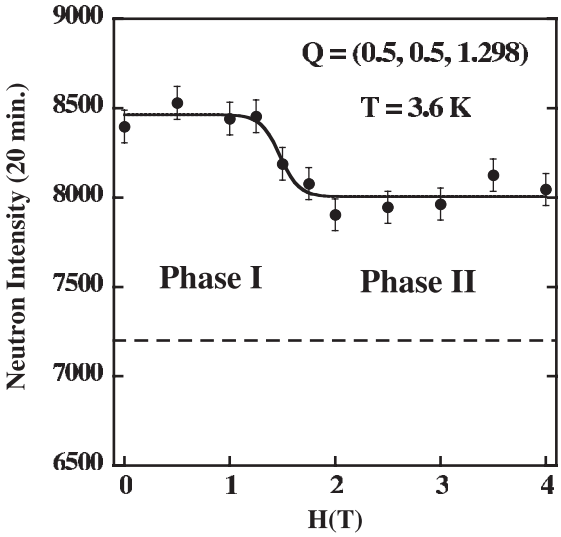

Figure 4. Magnetic field dependence of the Bragg peak intensity at $\mathbf{Q} = (0.5, 0.5, 1.298)$ at 3.6 K. The solid line is a guide for the eyes. The dashed line corresponds to the background.

Table 4. Magnetic refinement with a sine-wave structure in phase II for $H = 4$ T and $T = 3.6$ K. (Note: $R = 0.1902$.)

Q	$\lvert\mathbf{F}_{M\perp}(\mathbf{Q})\rvert^2_{calc}$	$\lvert\mathbf{F}_{M\perp}(\mathbf{Q})\rvert^2_{obs}$
$(1, 1, 0)-$	0.04	0.07 (0.03)
$(0, 0, 1)+$	0.31	0.21 (0.06)
$(1, 1, 1)-$	0.16	0.19 (0.03)
$(1, 1, 2)-$	0.36	0.37 (0.04)

this phase is that it exists in a reduced temperature range in the vicinity of the Néel temperature, where the magnetic moment is barely developed. As a consequence, the magnetic signal is weak. Figure 4 shows the field dependence of the magnetic Bragg peak intensity measured at $\mathbf{Q} = (1/2, 1/2, 1.298)$ at 3.6 K. Since the intensity is constant in both phases, this suggests that the propagation vector does not change as a function of field. Because of the weak signal, only four magnetic reflections were collected in phase II at 3.6 K and 4 T, and the result of a refinement with a sine-wave structure is given in table 4. For $H = 4$ T and $T = 3.6$ K, the magnetic amplitude is found to be $A_{II} = 0.44(2)\ \mu_B$. Refinement with an elliptical phase is slightly better ($R = 0.1449$ instead of $R = 0.1902$) and gives a non-zero component along the field, $m_{[1,\bar{1},0]} = 0.12(5)\ \mu_B$, the component perpendicular to the field being then $m_{[1,1,0]} = 0.41(5)\ \mu_B$. We cannot definitively conclude on the elliptical nature of this phase given the small number of collected reflections.

In the previous paragraphs, we neglect the possible ferromagnetic component along the applied field. The corresponding signal was not observed in the present experiment due to its location on the top of the nuclear peaks. The resulting structure obtained by combining the sine-wave and the ferromagnetic component is a so-called fan structure. The fact that m_{III} and m_I are equal within the error bars indicates that this ferromagnetic component is anyway very weak, at least at low temperature. Magnetization measurements performed at 1.3 K in the basal plane give an induced ferromagnetic moment of about 0.08 μ_B at 5 T [19]. The

helicoidal nature of the ordering at zero field is certainly due to the RKKY interactions that allow the conditions for stabilizing such a state due to their oscillating nature. We invoke RKKY interactions rather than Fermi surface nesting because dHvA experiments suggest the localized nature of the magnetism of $CeRhIn_5$ at ambient pressure [20]. The effect of a magnetic field applied in the plane of a helix has been known for a long time and was worked out shortly after the discovery of the helix structure [21]. The resulting sinusoidal oscillating structure or elliptical arrangement depends on the anisotropy and the magnetic field and the details of the complete (T, H) phase diagram depend on the precise Hamiltonian. The possible transition from a helix to a commensurate structure under field was also predicted in the earlier mean field approximation studies for particular values of the propagation vectors [22]. A field induced transition to the antiferromagnetic state is expected for $k \approx 1/2$ and to the $++--$ structure for $k \approx 1/4$, the situation encountered in the present work.

Despite the proximity of the zero-field propagation vector to that of the $++--$ structure, another commensurate structure is reported at zero field for doped $CeRhIn_5$ systems, with this time $\mathbf{k} = (1/2, 1/2, 1/2)$. This antiferromagnetic order occurs in $CeRh_{1-x}Ir_xIn_5$ ($0.25 \leqslant x \leqslant 0.6$) [23] and in $CeRh_{0.6}Co_{0.4}In_5$ [24]. Interestingly, it is reported to coexist with the incommensurate order and also with the superconducting ground state. On cooling the incommensurate order appears first followed by the commensurate order and the superconducting state. On the other hand, it is worthwhile to note that the commensurate order with $\mathbf{k} = (1/2, 1/2, 1/2)$ alone is reported for the related $CeCoIn_5$ compound doped with 10% Cd in the antiferromagnetic phase, including the low temperature region where antiferromagnetic order and superconductivity coexist [25]. Contrastingly, the occurrence of commensurate order is not reported in the diffraction studies performed on $CeRhIn_5$ under pressure. However, different groups obtain different results. Either the incommensurate order is reported to change weakly with pressure up to 1.63 GPa [26] or, in contrast, the propagation vector changes to $\mathbf{k} = (1/2, 1/2, 0.396)$ at 0.1 GPa [14]. This confusing situation requires new experiments under pressure. The occurrence of different commensurate and incommensurate phases in the (T, H, p, x) phase diagram of $CeRhIn_5$ deserves further investigation, especially for the interplay between magnetic order and superconductivity.

We have determined the two different magnetic ordering states in $CeRhIn_5$ at ambient pressure under magnetic field applied in the basal plane. The low temperature phase is characterized by the commensurate propagation vector $\mathbf{k} = (1/2, 1/2, 1/4)$ and a collinear structure with the magnetic moment perpendicular to the field. The saturated magnetic moment of 0.6 μ_B is the same as the one found in the zero-field phase. The high temperature phase is incommensurate, with the same propagation vector as the zero field incommensurate helix, $\mathbf{k} = (1/2, 1/2, 0.298)$. The structure is collinear at first approximation, with a possible ellipticity of about 1/3.

Acknowledgment

We acknowledge M Zhitomirsky for illuminating discussion concerning helicoidal structures under applied magnetic field.

References

[1] See e.g. Flouquet J 2005 *Prog. Low. Temp. Phys.* **15** 139
[2] See e.g. Mathur N D *et al* 1998 *Nature* **394** 39
[3] Demler E, Hanke W and Zhang S C 2004 *Rev. Mod. Phys.* **76** 909
[4] Kitaoka Y *et al* 2001 *J. Phys.: Condens. Matter* **13** L79

[5] See e.g. Thompson J D *et al* 2001 *J. Magn. Magn. Mater.* **226–230** 5
[6] Park T *et al* 2006 *Nature* **440** 65
[7] Knebel G *et al* 2006 *Phys. Rev.* B **74** 020501(R)
[8] Chen G F *et al* 2006 *Phys. Rev. Lett.* **97** 017005
[9] Kawasaki S *et al* 2003 *Phys. Rev. Lett.* **91** 137001
[10] Moschopoulu E G *et al* 2002 *Appl. Phys.* A **74** (Suppl.) 5895
[11] Cornelius A L *et al* 2001 *Phys. Rev.* B **64** 144111
[12] Correa V F *et al* 2004 *Preprint* cond-mat/0411359.s
[13] Bao W *et al* 2000 *Phys. Rev.* B **62** R14621
Bao W *et al* 2003 *Phys. Rev.* B **67** 099903 (erratum)
[14] Majumdar S *et al* 2002 *Phys. Rev.* B **66** 212502
[15] Curro N J *et al* 2000 *Phys. Rev.* B **62** R6100
[16] Wolfers P 1990 *J. Appl. Crystallogr.* **23** 554
[17] Becker P J and Coppens P 1974 *Acta Crystallogr.* A **30** 129
[18] Christianson A D *et al* 2002 *Phys. Rev.* B **66** 193102
[19] Takeuchi T *et al* 2001 *J. Phys. Soc. Japan* **70** 877
[20] Onuki Y *et al* 2003 *Acta Phys. Pol.* B **34** 667
[21] Nagamiya T 1967 *Solid State Phys.* vol 20 (New York: Academic) p 305 and references therein
[22] See e.g. Nagamiya T *et al* 1962 *Prog. Theor. Phys.* **27** 1253
[23] Christianson A D *et al* 2005 *Phys. Rev. Lett.* **95** 2117002
[24] Yokoyama M *et al* 2006 *J. Phys. Soc. Japan* **75** 103703
[25] Nicklas M *et al* 2007 *Preprint* cond-mat/0703703
[26] Llobet A *et al* 2004 *Phys. Rev.* B **69** 024403